MICROSTRUCTURAL EVOLUTION AND MECHANICAL PERFORMANCE OF SMAW DISSIMILAR WELDS BETWEEN ASTM A36 AND AISI 316 WITH E316-16 ELECTRODE AT DIFFERENT WELDING CURRENTS

NURHABIBAH PARAMITHA EKA UTAMI*, DIAH KUSUMA PRATIWI,
HENDRI CHANDRA, ASTUTI, ELLYANIE , WISNU HAFIZ PRASTYANTO,
MUHAMMAD IHSAN RIADY, DYOS SANTOSO, M. A. ADE SAPUTRA

Department of Mechanical Engineering, Universitas Sriwijaya, South Sumatra, Indonesia

**Corresponding author: nhparamitha@ft.unsri.ac.id*

(Received: 3 September 2025; Accepted: 10 November 2025; Published on-line: 1 December 2025)

ABSTRAK: This study investigates the effect of welding current on the microstructural evolution and mechanical performance of Shielded Metal Arc Welded (SMAW) dissimilar lap joints between ASTM A36 carbon steel and AISI 316 stainless steel using an E316-16 electrode. Welding was performed at three different currents, namely 60 A, 70 A, and 80 A, to evaluate their influence on microstructure, hardness distribution, and impact toughness. Microstructural characterization was conducted using optical microscopy to examine phase formation and grain morphology in the weld metal and heat-affected zone (HAZ). Mechanical properties were evaluated through Vickers hardness testing and Charpy impact testing. The results show that increasing welding current leads to higher heat input, promoting the formation of finer pearlite and acicular ferrite in the weld metal, along with an expansion of the HAZ. These microstructural changes resulted in increased hardness, with the highest average hardness value of 343.32 HV observed in the weld metal at 80 A. Impact test results indicated that higher welding currents enhanced impact toughness due to the interlocking morphology of acicular ferrite, which effectively retards crack propagation. However, localized grain coarsening was observed near the fusion boundary, particularly within the HAZ. Overall, a welding current of 80 A provided the most favorable combination of hardness and impact toughness, indicating its suitability for optimizing the mechanical performance of SMAW dissimilar welded joints between ASTM A36 and AISI 316.

KEY WORDS: Dissimilar metal welding; SMAW; Welding current; Microstructure; Mechanical properties; E316-16 electrode

1. INTRODUCTION

Dissimilar metal welding is widely employed in industrial applications such as pressure vessels, piping systems, and heat exchangers, where materials with different properties are combined to achieve optimal performance and cost efficiency [1]. The combination of ASTM A36 and AISI 316 steel is particularly attractive due to the good weldability and low cost of carbon steel, together with the excellent corrosion resistance and ductility of stainless steel. However, joining these dissimilar materials presents significant metallurgical challenges arising from differences in chemical composition, thermal conductivity, and phase transformation behavior during welding. Shielded Metal Arc Welding (SMAW) remains one of the most commonly used welding processes for structural and fabrication applications because of its simplicity, versatility, and economic advantages [2]. Among the welding parameters, welding current plays a critical role in controlling heat input, penetration depth,

cooling rate, and microstructural evolution in the weld metal and heat-affected zone (HAZ) [3]. Variations in welding current can significantly influence phase formation, grain morphology, and defect formation, which in turn affect the mechanical performance of welded joints [4]. The selection of an appropriate filler metal is equally important in dissimilar metal welding. The E316-16 electrode is commonly used for joining carbon steel to austenitic stainless steel due to its compatibility, enhanced corrosion resistance, and ability to accommodate compositional dilution effects. Despite its industrial relevance, systematic studies examining the combined influence of welding current and E316-16 filler metal on the microstructural evolution and mechanical behavior of SMAW dissimilar welds between ASTM A36 and AISI 316 remain limited. Therefore, this study aims to investigate the effect of different welding currents on the microstructural evolution and mechanical performance of SMAW dissimilar welded joints between ASTM A36 and AISI 316 using an E316-16 electrode. Microstructural observations are conducted to analyze phase distribution and grain evolution in the weld metal and HAZ, while mechanical testing is performed to evaluate hardness and joint performance. The findings of this study are expected to provide valuable insights for optimizing welding parameters in dissimilar metal joining applications.

2. RESEARCH METHODS

The materials used in this study were ASTM A36 and AISI 316 steel in plate form. Dissimilar lap joints were fabricated using SMAW with an E316-16 electrode. Three types of welding currents were employed, which are 60 A, 70 A and 80 A to evaluate their influence on the mechanical and microstructural characteristics of the welded joints. All welding procedures were conducted in accordance with the American Welding Society (AWS) standards to ensure process consistency and to minimize welding defects. Welding Geometry can be seen in Figure 1. Chemical composition of ASTM A36 and AISI 316 is shown in Table 1 and Table 2, while mechanical characteristics of ASTM A36 and AISI 316 are shown in Table 3 and Table 4. Chemical composition of E316-16 can be seen in Table 5.

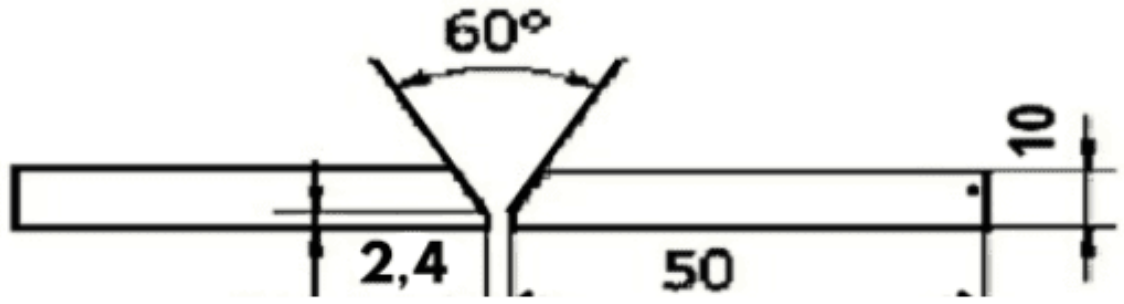

Fig. 1. Welding Geometry

Table 1: Chemical Composition of ASTM A36

Element	C	Si	Mn	Cr	Ni	Al	S	V
(%)	0.17	0.24	0.73	0.01	0.03	0.01	0.009	0.003
Element	Mo	Cu	Nb	Ti	N	P	CE	Fe
(%)	0.002	0.04	0.002	0.006	0.02	0.015	0.28	Balance

Table 2: Chemical Composition of AISI 316

Element	C	Ni	Mn	Cr	Si	S	P
(%)	0.029	9.930	1.648	16.86	0.39	0.035	0.050

Table 3: Mechanical Characteristics of ASTM A36

Yield Stress [MPa]	UTS [MPa]	Strain in 2 inches [50 mm], %
250	400-500	23

Table 4. Mechanical Characteristics of AISI 316

Yield Stress Min, ksi [MPa]	UTS Ksi [MPa]	Strain in 2 inches [50 mm], %
205	515	40

Table 5: Chemical Composition E316-16

Element	C	Ni	Mn	Cr	Si	S	P	Mo	Cu
(%)	0.04	12.0	1.5	19.2	0.35	0.01	0.03	2.2	0.10

Prior to welding, the plate surfaces and groove areas were thoroughly cleaned to remove oil, dust, and other contaminants. The specimens were fixed using tack welding to prevent distortion during welding. Welding was performed under controlled environmental conditions, avoiding excessive humidity and air flow. After welding, the specimens were stored in a dry environment to prevent corrosion. Microstructural analysis was carried out using standard metallographic techniques. Welded specimens were sectioned, mounted, ground, polished, and chemically etched prior to microscopic observation. Different etching solutions were used for each base material: a 2% nitric acid solution in alcohol for ASTM A36 and a mixed solution of hydrofluoric acid, nitric acid, and distilled water for AISI 316. The microstructures of the weld metal, heat-affected zone (HAZ), and base metals were examined to identify phase formation and microstructural changes resulting from the welding process. Mechanical characterization included Vickers hardness testing and impact tests. Hardness measurements were performed using a Vickers hardness tester in accordance with JIS Z 2244 standards to evaluate hardness distribution across the welded joint. Impact tests were conducted using a Charpy impact testing machine following JIS B 7722 standards to assess the impact strength and overall mechanical performance of the dissimilar welded joints.

3. RESULTS AND DISCUSSION

3.1. Microstructure Analysis

Optical microscopy was conducted to examine the microstructural features of each specimen. This analysis aimed to identify grain size, phase distribution, and characteristic

microstructural features of the materials. Prior to observation, the specimens were etched using a nital solution for ASTM A36 and aqua regia for SS 316 to reveal the microstructural details. The microstructures of the ASTM A36 and AISI 316 base metals are presented in Figure 2.

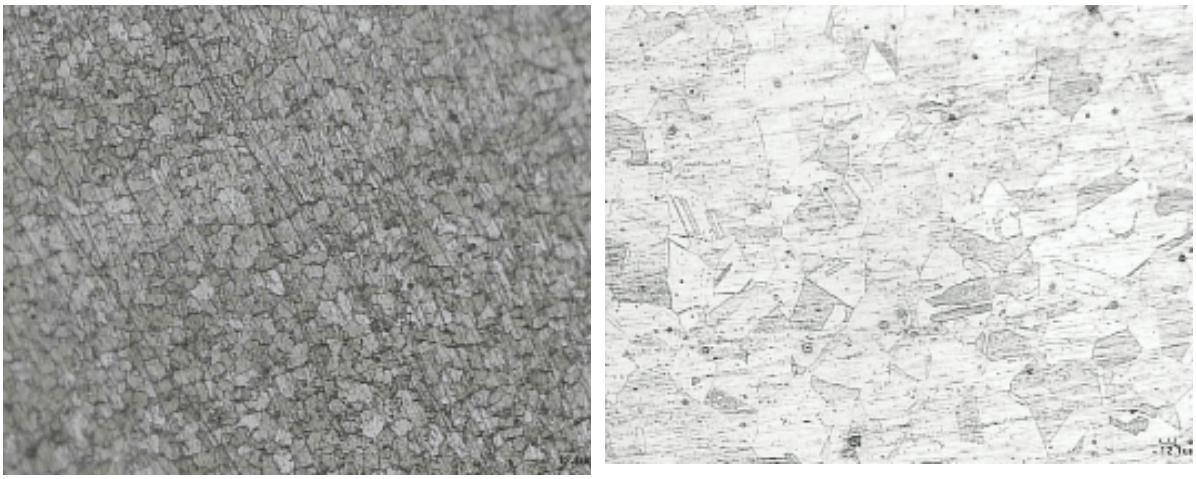

(a) (b)

Fig. 2. The Microstructure of base metals (a) ASTM A36 (b) AISI 316

Figure 3 shows that the morphology of ferrite and pearlite in the heat-affected zone (HAZ) differs from that observed in the base metal region. This microstructural variation is attributed to the thermal cycle experienced during the welding process. An increase in heat input leads to a wider HAZ due to prolonged exposure to elevated temperatures. In the stainless steel HAZ, the formation of Widmanstätten ferrite was observed, which is associated with relatively slow cooling rates from high temperatures. Widmanstätten ferrite is characterized by high hardness, while bainitic structures exhibit good toughness. The combined presence of these microstructural constituents contributes to improved toughness of the welded joint.

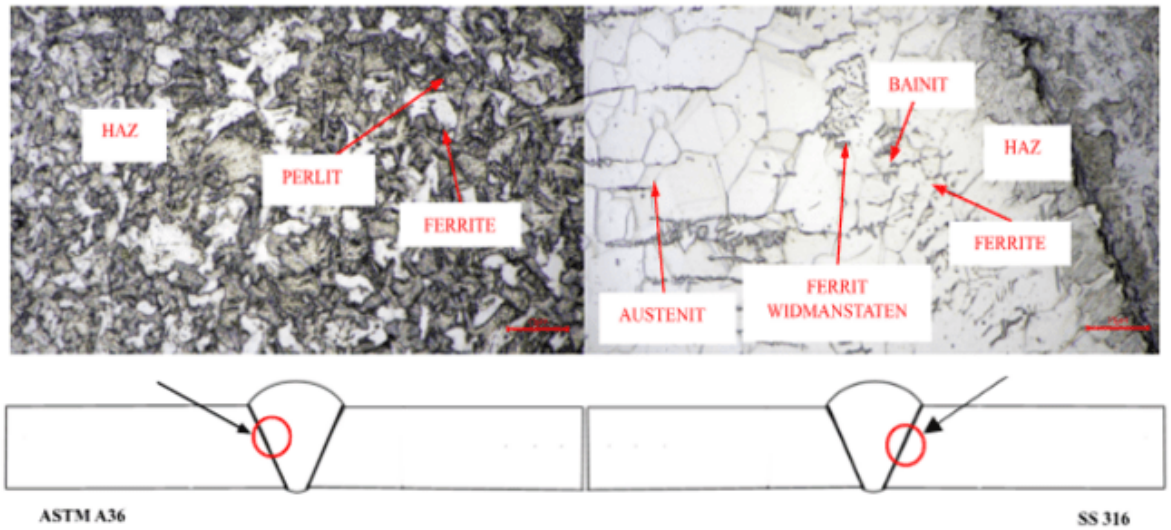

(a)

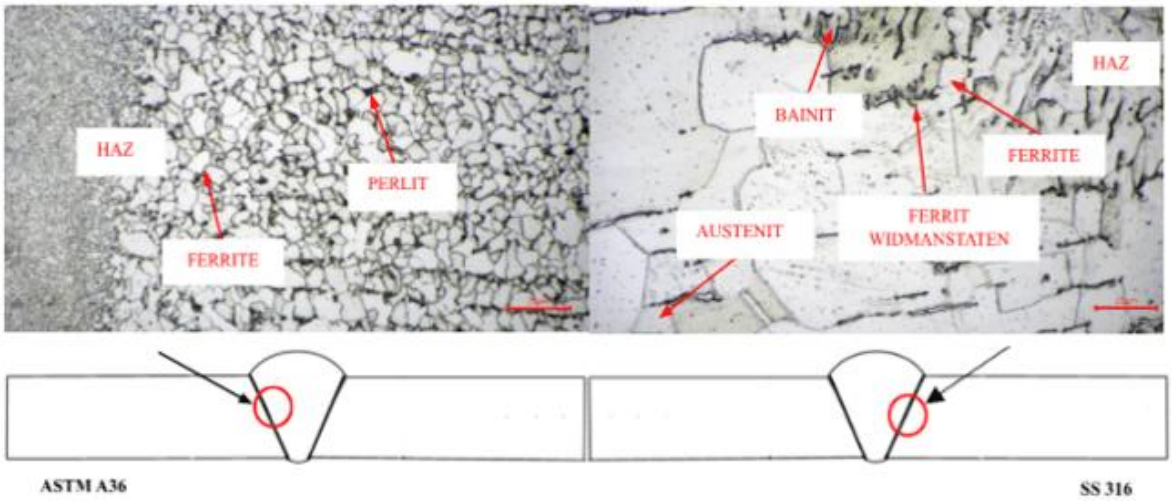

(b)

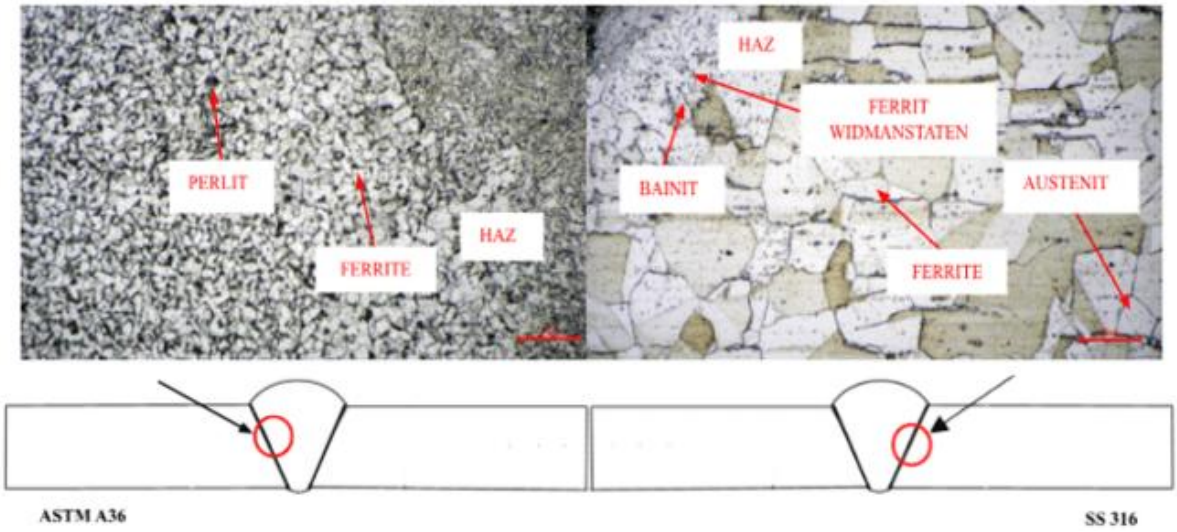

(c)

Fig. 3. HAZ of Dissimilar welded (a) 60 A (b) 70 A (c) 80 A

Based on the observations presented in Figure 4, a clear correlation can be identified between the microstructural characteristics and the hardness test results. An increase in welding current leads to a higher fraction of pearlitic microstructure, accompanied by an increase in hardness values [5]. This behavior is attributed to the formation of finer microstructural constituents, as finer pearlite is known to enhance the hardness of steel. The application of higher welding currents also results in increased heat input, which influences phase formation and promotes the development of acicular ferrite in the weld metal [6]. A higher proportion of acicular ferrite can retard crack propagation due to its interlocking morphology, thereby improving the toughness of the welded joint [7]. However, excessive heat input may also cause grain coarsening in the weld metal region, as evidenced by the coarser grain morphology observed, resulting from prolonged exposure to elevated temperatures during welding [8].

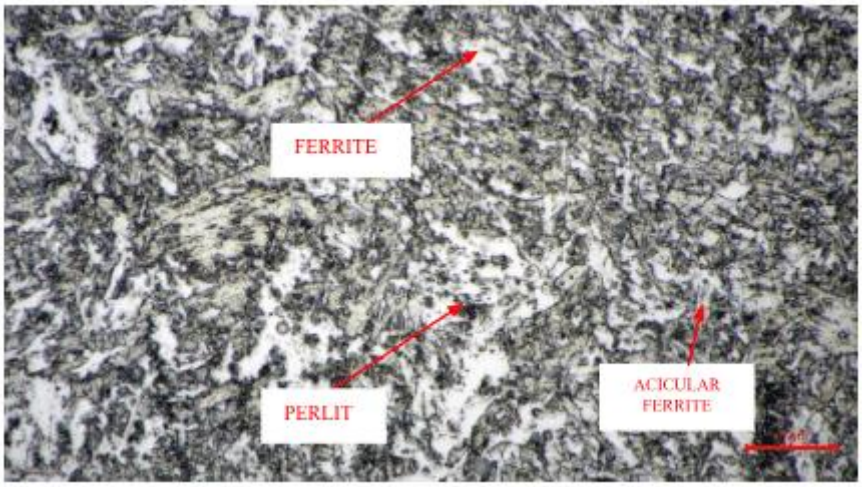

(a)

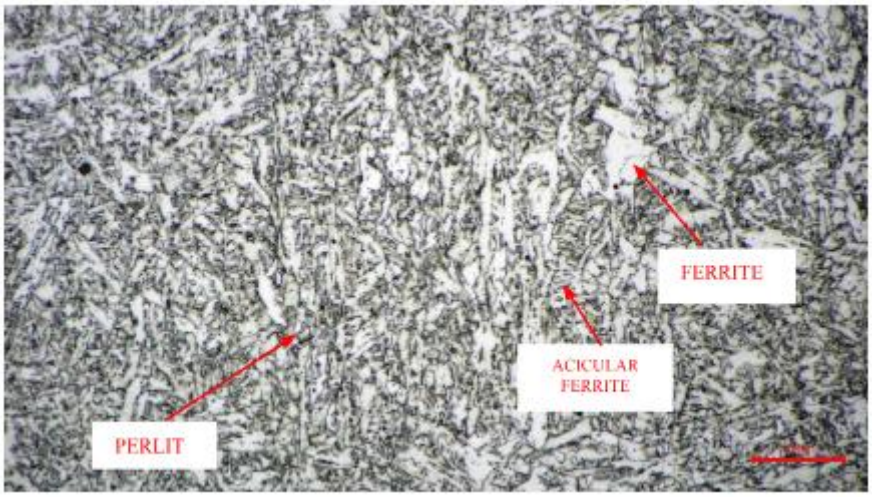

(b)

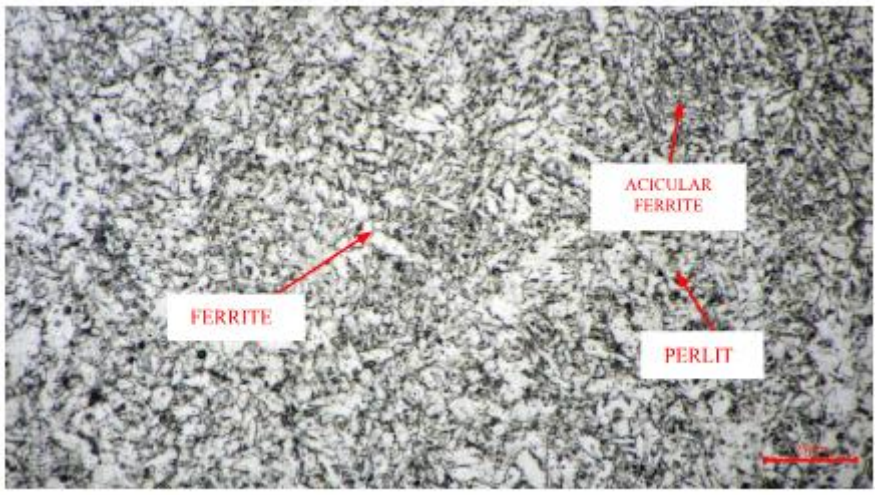

(c)

Fig. 4. Weld metal of Dissimilar welded (a) 60 A, (b) 70 A, (c) 80 A

3.2. Hardness Analysis

Hardness testing was performed using the Vickers method in accordance with ASTM E92 to evaluate the effect of welding current on hardness distribution (Figure 5). The tests were

conducted with a load of 30 kgf and a dwell time of 10 s, with measurements taken at five locations in the ASTM A36 base metal, AISI 316 base metal, weld metal, and heat-affected zone (HAZ). The highest average hardness was obtained at a welding current of 80 A in the weld metal region (343.32 HV), while the lowest value was recorded at 60 A (219.40 HV). An increasing welding current resulted in higher hardness values, which is attributed to increased heat input affecting cooling rates and microstructural morphology. The relatively lower hardness in the HAZ compared to the weld metal is associated with grain coarsening near the fusion boundary due to thermal exposure from the weld metal [9].

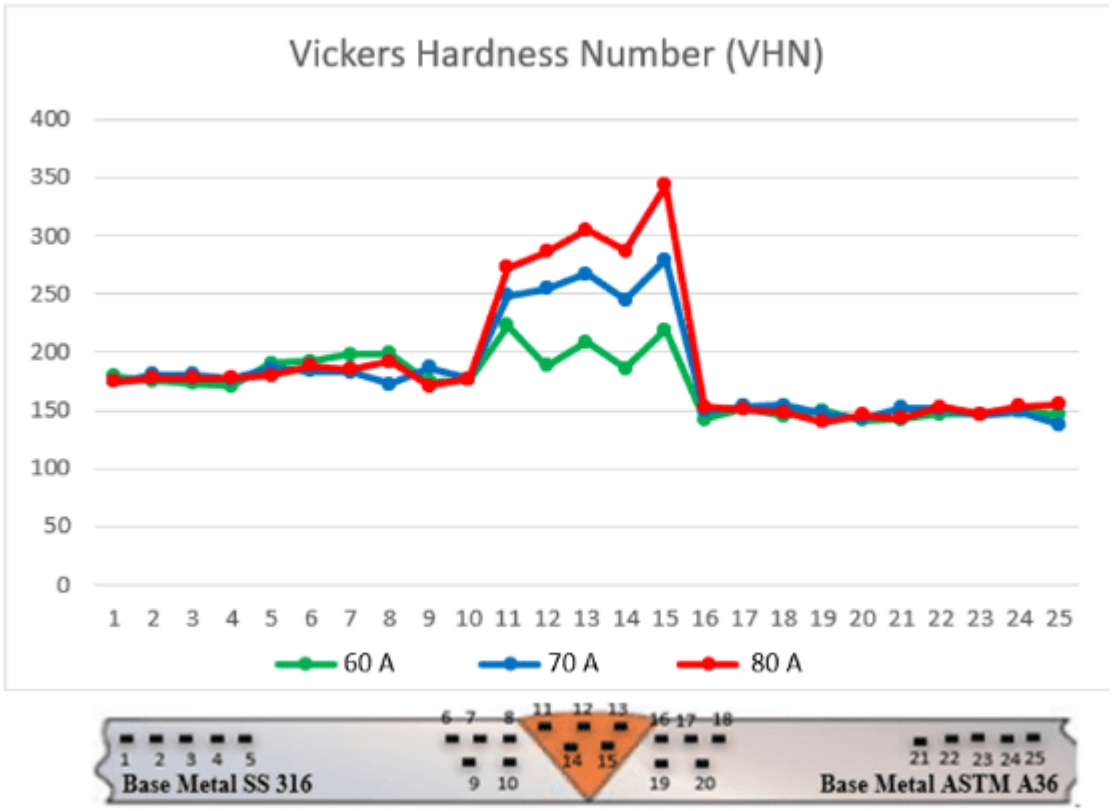

Fig. 5. Vickers hardness number of dissimilar weld of ASTM A36 and AISI 316

3.3. Impact Analysis

Impact testing was conducted using the Charpy method in accordance with ASME Section IX. The test apparatus employed a pendulum with a mass of 25.68 kg, a distance of 0.649 m from the center of gravity, a gravitational acceleration of 9.8 m/s², and an initial angle (α) of 146.5°. For each welding parameter, three specimens were tested with the notch positioned in the weld metal. The average values were used to determine the final pendulum angle (β), absorbed impact energy, and impact toughness. The impact test results are summarized in Table 6, while the average impact energy is illustrated in Figure 6.

Table 6: The impact test results

Specimens	*β* angle	Energy *(Joule)*
60 A	62.5	211,62
	83	156,10
	62.5	211,62
70 A	62	212,88
	70	192,06
	50	241,18
80 A	51	238,99
	77	172,94
	46	249,66

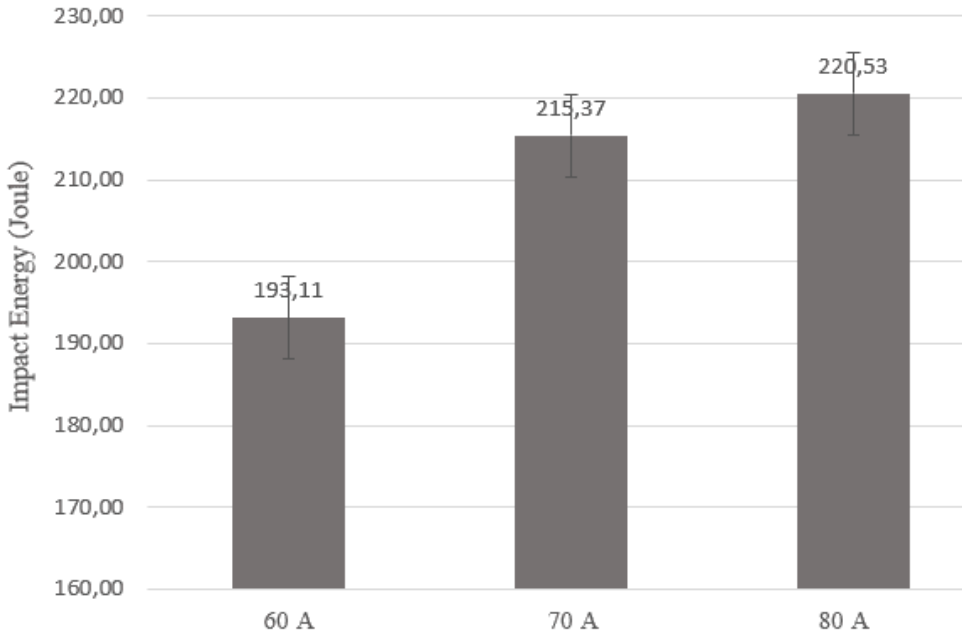

Fig. 6. Average impact energy

As shown in Figure 4.4, the highest impact energy was obtained at a welding current of 80 A, reaching 220.53 J/mm², while the lowest value was recorded at 60 A, with an impact energy of 193.11 J/mm². The impact toughness measured in the weld metal region indicates that variations in welding current have a significant influence on the toughness of the welded joint. Higher welding currents increase the heat input during the welding process, resulting in a slower cooling rate and promoting the formation of acicular ferrite. This microstructural feature effectively retards crack propagation, thereby enhancing the impact toughness of the weld metal [10].

4. CONCLUSIONS

The results demonstrate that welding current significantly influences heat input, microstructural characteristics, and mechanical properties of the welded joints. Increasing the

welding current from 60 A to 80 A promoted the formation of finer pearlite and acicular ferrite in the weld metal, while also enlarging the heat-affected zone due to prolonged thermal exposure. These microstructural changes led to an increase in hardness, with the highest hardness value recorded in the weld metal at 80 A. Impact test results further confirmed that higher welding currents enhanced impact toughness, which is attributed to the interlocking morphology of acicular ferrite that effectively retards crack propagation. However, localized grain coarsening was observed near the fusion boundary, particularly in the HAZ, resulting in relatively lower hardness compared to the weld metal. Overall, a welding current of 80 A provided the most favorable balance between hardness and impact toughness, indicating its suitability for optimizing the mechanical performance of SMAW dissimilar welded joints between ASTM A36 and AISI 316. The findings of this study contribute to a better understanding of welding parameter optimization in dissimilar metal welding applications.

REFERENCES

[1] D. K. Pratiwi, A. Arifin, Gunawan, A. Mardhi, and Afriansyah, "Investigation of Welding Parameters of Dissimilar Weld of SS316 and ASTM A36 Joint Using a Grey-Based Taguchi Optimization Approach," *Journal of Manufacturing and Materials Processing*, vol. 7, no. 1, p. 39, Feb. 2023, doi: 10.3390/jmmp7010039.

[2] R. Akbar, J. Awali, F. Stasiyanur, and M. P. D. Lubis, "Analysis of the Effect of Variations in Welding Current of the Combination of SMAW & FCAW Using Double V Groove on Tensile Strength, Impact and Microstructure in ASTM A36 Steel Weld Metal Area," *SPECTA Journal of Technology*, vol. 7, no. 1, May 2023, doi: 10.35718/specta.v7i1.704.

[3] T. Teker and D. Gencdogan, "Heat affected zone and weld metal analysis of HARDOX 450 and ferritic stainless steel double sided TIG-joints," *Materials Testing*, vol. 63, no. 10, pp. 923–928, Oct. 2021, doi: 10.1515/mt-2021-0022.

[4] A. D. Gandhi, A. Kundu, R. Kumar, and P. C. Chakraborti, "Effect of Heat Input on the Weld Thermal Cycle, Microstructure, Tensile Damage and Fracture Behavior of Pulsed Laser-Welded Dual-Phase Steel," *J Mater Eng Perform*, vol. 33, no. 23, pp. 13049–13066, Dec. 2024, doi: 10.1007/s11665-023-08377-4.

[5] H. Karabulut, M. Türkmen, M. Erden, and S. Gündüz, "Effect of Different Current Values on Microstructure and Mechanical Properties of Microalloyed Steels Joined by the Submerged Arc Welding Method," *Metals (Basel)*, vol. 6, no. 11, p. 281, Nov. 2016, doi: 10.3390/met6110281.

[6] L. Wang, Y. Jiang, C. Hu, X. Wan, and G. Li, "Effect of heat input on microstructure evolution and fracture toughness of interlayer heat affected zone in ultra-high strength steel," *Journal of Materials Research and Technology*, vol. 39, pp. 5189–5198, Nov. 2025, doi: 10.1016/j.jmrt.2025.10.201.

[7] D. REN, "Effects of welding wire composition and welding process on the weld metal toughness of submerged arc welded pipeline steel," *International Journal of Minerals, Metallurgy and Materials*, vol. 16, no. 1, pp. 65–70, Feb. 2009, doi: 10.1016/S1674-4799(09)60011-X.

[8] Z. H. Xia, X. L. Wan, X. L. Tao, and K. M. Wu, "Effect of Heat Input on Toughness of Coarse-Grained Heat-Affected Zone of an Ultra Low Carbon Acicular Ferrite Steel," *Adv Mat Res*, vol. 538–541, pp. 2003–2008, Jun. 2012, doi: 10.4028/www.scientific.net/AMR.538-541.2003.

[9] R. Dhairiyasamy, D. Gabiriel, M. Kandasamy, and S. Rajendran, "Investigation of Microstructural and Mechanical Characteristics of Friction Stir Welded Aluminum Alloy 7075-t6," *Transactions of the Indian Institute of Metals*, vol. 77, no. 11, pp. 3789–3797, Nov. 2024, doi: 10.1007/s12666-024-03423-8.

[10] F. Song, C. Yin, F. Hu, and K. Wu, "Effects of Mn-Depleted Zone Formation on Acicular Ferrite Transformation in Weld Metals under High Heat Input Welding," *Materials*, vol. 15, no. 23, p. 8477, Nov. 2022, doi: 10.3390/ma15238477.